

A New ac Electro spray Mechanism by Maxwell-Wagner Polarization and Capillary Resonance

Leslie Y. Yeo, Dmitri Lastochkin, Shau-Chun Wang,* and Hsueh-Chia Chang

Center for Microfluidics and Medical Diagnostics, Department of Chemical and Biomolecular Engineering,
University of Notre Dame, Notre Dame, Indiana 46556, USA

(Received 31 October 2003; published 1 April 2004)

We report a new high-frequency (> 10 kHz) ac electro spray that is capable of generating micron-sized electroneutral drops. Unlike its dc counterpart, the drops are not ejected continuously from a sharp Taylor cone but intermittently from a resonating meniscus at the orifice. We attribute the resonant frequency to the capillary-inertia vibration time of the meniscus and the drop ejection to the Maxwell-Wagner electric stress at the drop tip, which is observed to reverse its direction across a crossover frequency. Above this frequency, the oppositely directed Maxwell-Wagner force causes the liquid to recede up the microneedle as an apparent electrowetting effect.

DOI: 10.1103/PhysRevLett.92.133902

PACS numbers: 41.20.Cv, 47.20.Ma, 77.22.Ej

Electrospraying is commonly used for the production of fine mono- and polydispersed drops in widespread applications such as electro spray ionization mass spectrometry for protein and DNA characterization [1], respiratory drug delivery [2], microencapsulation, etc. Electro spraying, in general, employs the principle in which the applied electrical stress stretches the liquid meniscus at the capillary tip which subsequently deforms and breaks off. With the exception of a few recent studies, the majority of work has focused on dc fields [3]; the few ac studies available have been limited to either dc superimposed ac fields [4] or low ac frequencies [5]. In this Letter, we report a new electro spray phenomenon in which micron-sized ethanol drops are generated at high ac frequencies (10–280 kHz). The spray modes observed, as well as the electroneutrality and dimensions of the drops produced, are distinct to that in dc electro spraying, thus extending the use of electro sprays to a wider area of possible application. We shall proceed by describing the experimental setup and observations, followed by an attempt to elucidate the various complex spray phenomena observed by employing simple scaling arguments.

The experimental apparatus is schematically described in Fig. 1. A metal hub microneedle (Hamilton N733) with nominal outer diameter 0.21 mm and thickness 0.05 mm, mounted at 50° to the horizontal, is connected to a high voltage output transformer (Industrial Test Equipment) and rf amplifier (Powertron 250 A, 10 Hz–1 MHz), capable of delivering up to 6000 V (peak to peak) and 250 W; ac frequencies were produced by a function/arbitrary waveform generator (Hewlett-Packard 33120A). The ground electrode consisted of a strip of copper tape placed 5 mm away from the needle tip. Spray development was imaged using a high speed video camera (Kodak Ektapro 1000 Imager and High-Spec Processor) at record rates of 1000–6000 frames/s, connected to a telescopic lens to achieve an overall magnification of $800\times$; background illumination was provided by a fiber-optic lamp (Fiber-Lite PL-800). The

working liquid is 95% ethanol (AAPER Alcohol & Chemical Co. 190 Proof), with interfacial tension $\sigma \sim 25$ mN/m, density $\rho \sim 816$ kg/m³, viscosity $\mu \sim 1.2$ mPa s, conductivity $\kappa \sim 4 \times 10^{-5}$ S/m, and relative permittivity $\epsilon_r = 24.3$.

Figure 2 depicts the delineation between the various spray regimes observed as a function of both the applied frequency, f , and the applied peak-to-peak voltage, V . In all cases, the flights of the ejected micron-sized drops do not follow the field lines; the drops can also be easily deflected by cross flow. In addition, the current arising from the charge carried by the drops was undetectable due to the presence of background ac current. Thus, unlike dc electro sprays, the drops are believed to be electroneutral. Perhaps the most fundamental observation of the high-frequency ac electro spray modes in our experiments is the absence of a well-defined Taylor cone (formation of a conical meniscus with a half angle close to the Taylor angle of 49.3°), which is primarily characteristic of the predominant stable cone-jet mode in dc electro sprays [3]. In addition, none of the other dc electro spray modes such as dripping, intermittent cone jet, ramified jet, or spindle modes [3] are observed. Instead, the meniscus is seen to resonate at some characteristic

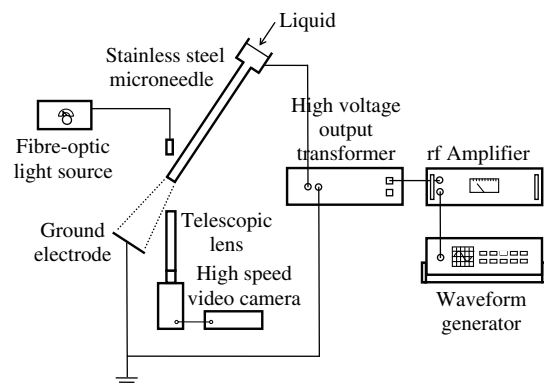


FIG. 1. Schematic illustration of the experimental setup.

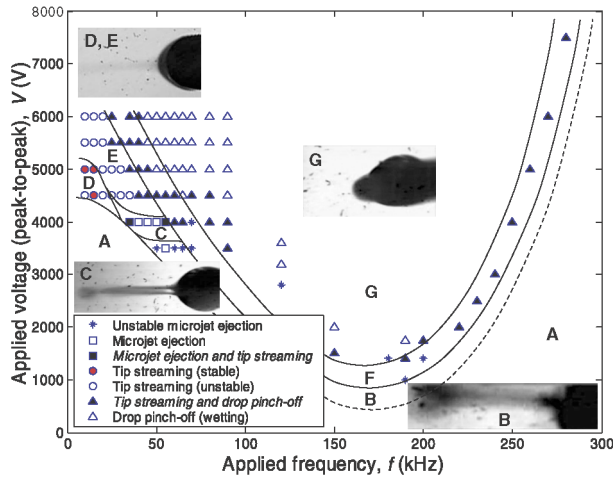


FIG. 2 (color online). Pattern map illustrating the various ac electro spray regimes: (A) capillary dominant regime (no drop ejection); (B) unstable microjet ejection; (C) microjet ejection with/without tip streaming; (D) stable tip streaming; (E) unstable tip streaming; (F) tip streaming with drop pinch-off (onset of wetting); and (G) drop pinch-off (wetting).

frequency, $f_1 \sim 10$ Hz, periodically ejecting drops with diameters estimated to be of order $10 \mu\text{m}$, either at the same characteristic frequency or at another distinct characteristic frequency, $f_2 \sim 10^3$ Hz. However, drop ejection is limited to a voltage window, which is a function of f . Below this window, there is insufficient electrical force to overcome the capillary force at the tip of the meniscus. Above the window, wetting is observed to draw liquid up the needle. The low frequency ejection mode resembles drop pinch-off due to wetting effects, tip streaming [6] from a transient cone or a microjet that forms intermittently from the resonating meniscus at frequency f_1 . The high-frequency mode involves the ejection of single or multiple drops at the end of the tip or microjet at frequency f_2 . The multiple spray modes and the biperiodic behavior observed thus indicate the influence of several competing and interacting physical effects on the drop.

A candidate for the driving electric force is the ac Maxwell stress due to field-induced double layer polarization at the interface [7]. From the liquid conductivity, an ionic concentration, c , of roughly 10^{-7} M is obtained, from which we deduce the double layer thickness, $\lambda = [(\epsilon_l R_g T_l)/(2F^2 z^2 c)]^{1/2}$, to be approximately $0.2 \mu\text{m}$, ϵ_l being the liquid permittivity ($\epsilon_l = \epsilon_r \epsilon_o$ where ϵ_o is the

vacuum permittivity), R_g the molar gas constant, T_l the absolute temperature, F the Faraday constant, and z the ionic valency. This relatively thick double layer translates into a Debye diffusion time, $T_d \sim \lambda^2/\mathcal{D}$, of 10^{-3} s, \mathcal{D} being the ionic diffusivity, which is larger than the period of the applied ac field, T . Moreover, if ac charging of the double layer were to be the responsible mechanism for the polarization, the spray regimes observed would be very sensitive to the double layer thickness and hence the ionic concentration. Nevertheless, the use of ethanol with lower ionic concentrations as well as the addition of 1 ppm hydrochloric acid to increase the ionic concentration, so that the conductivities varied between 10 to 100 times in either direction, did not yield a significant quantitative or qualitative difference in the results. This is due to the large time scale for bulk ionic diffusion, R^2/\mathcal{D} , of 10^3 – 10^4 s, where R is the apparent length scale of the drop, taken to be 5 mm (approximated by factoring the drop curvature at the needle tip by 10 to account for the entire drop radius), compared to T .

A comparison of the drop viscous drainage times due to Maxwell-Wagner and double layer interfacial polarization, T_{MW} and T_{DL} , respectively, obtained via a balance of the relevant force ($F_{\text{MW}} \sim \text{Re}[f_{\text{CM}}]\epsilon_o|E_\infty|^2$ and $F_{\text{DL}} \sim QE_\infty R^{-2}$; $E_\infty \sim V/L$ is the applied field and $L \sim 5$ mm is the electrode separation) with viscous dissipation $\mu\mathcal{U}/R$ (see Table I), yields $T_{\text{DL}}/T_{\text{MW}} \sim \text{Re}[f_{\text{CM}}]\epsilon_o R^2 V Q^{-1} L^{-1} \sim 10^2$. Here, \mathcal{U} is the characteristic velocity and Q is the charge ($Q = cN_A e R^3$, where N_A is Avogadro's constant and e is the electronic charge). f_{CM} is the Maxwell-Wagner form of the Clausius-Mossotti polarization factor that allows for a reactive current:

$$f_{\text{CM}} = \frac{\tilde{\epsilon}_o - \tilde{\epsilon}_l}{\tilde{\epsilon}_l + 2\tilde{\epsilon}_o}. \quad (1)$$

$\tilde{\epsilon}$ indicates a complex permittivity given by $\tilde{\epsilon} = \epsilon - i(\kappa/\omega)$, where $i = \sqrt{-1}$; the subscripts l and o refer to the liquid and the ambient medium, respectively. The conductivity κ accounts for ion motion across the interface due to a gas-phase or interfacial liquid ionization reaction to be described subsequently. f_{CM} thus represents the dependence of the effective polarizability of the liquid on the angular frequency of the applied field $\omega (=2\pi f)$. Since $T_{\text{DL}} \gg T_{\text{MW}}$, and as $T_{\text{MW}} \sim T$, it is Maxwell-Wagner interfacial polarization that is responsible for the generation of the dipole moment at the

TABLE I. Typical length/time magnitudes for the relevant physical effects governing the dynamics of drop ejection.

Physical effect	Scaling	Magnitude
Viscous drainage time due to double layer polarization	$T_{\text{DL}} \sim \mu R^2 L Q^{-1} V^{-1}$	10^{-4} – 10^{-5} s
Viscous drainage time due to Maxwell-Wagner polarization	$T_{\text{MW}} \sim \mu L^2 \text{Re}[f_{\text{CM}}]^{-1} \epsilon_o^{-1} V^{-2}$	10^{-6} s
Maxwell-Wagner polarization-capillary force balance	$V_c \sim (\sigma L^2 f_{\text{CM}}^{-1} \epsilon_o^{-1} R^{-1})^{1/2}$	10^3 V
Viscous-capillary pinch-off time	$T_v \sim \mu R \sigma^{-1}$	2×10^{-5} – 5×10^{-5} s (jet)
Capillary-inertia pinch-off time	$T_i \sim (\rho R^3 \sigma^{-1})^{1/2}$	10^{-3} s (jet); 10^{-1} – 10^{-2} s (drop)

meniscus tip. Furthermore, the ratio of the instantaneous induced surface charge due to Maxwell-Wagner polarization, $\epsilon_o f_{CM} E_\infty$, to that due to ac double layer charging in one half cycle, $\kappa_l T E_\infty$, is approximately T_d/T since $T_d \sim \epsilon_o/\kappa_l$. For ethanol, $T_d/T \sim 10^3-10^4$, thus suggesting that double layer charging in the case of weak electrolytes is negligible. It can be seen that when $f \lesssim 10$ Hz, $T_d \lesssim T$ and hence double layer charging then becomes significant. An important consequence of this is that, in the absence of significant gas or interfacial liquid ionization, the drops produced by this mechanism are electroneutral, consistent with our observations, since the meniscus polarization is due to transient molecular dipoles at the tip that relaxes rapidly in the ejected drop. This is in contrast to double layer polarization in dc electrospays of electrolytes which produces drops with a permanent charge. Further support for the Maxwell-Wagner polarization mechanism lies in the existence of a critical drop ejection voltage, V_c . Balancing the Maxwell-Wagner force to the capillary force σ/R , we obtain $V_c \sim 10^3$ V (see Table I) in rough agreement with the lowest onset voltage at $f \sim 180$ kHz in Fig. 2.

Figure 3 depicts f_1 and f_2 by scanning along the drop ejection window. As f increases, the tip elongates to form a microjet suggesting an increase in inertial effects. An examination of the viscous-capillary pinch-off time [8] for the microjet in Table I indicates that viscous effects become significant at $f_v \sim 20-50$ kHz. f_v therefore forms the boundary between the microjet ejection and tip streaming modes. Above f_v , a long thread forms intermittently and microdrops are ejected by a microjet breakup mechanism due to capillary-inertial effects.

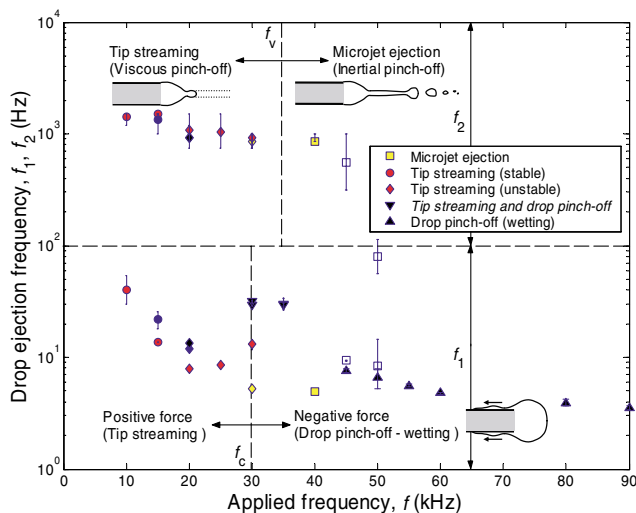


FIG. 3 (color online). Drop ejection frequency as a function of the applied ac frequency for various electrospay modes. The data points used are taken from a scan across the modes in the ejection window of Fig. 2; different shades for the plot markers are used to distinguish V : 4000–4500 V (no fill), 4500–5500 V (partial fill), and 5500–6000 V (complete fill).

Below f_v , intermittent tip streaming occurs at the resonant frequency due to a viscous-capillary pinch-off mechanism. The increasing viscous dominance suggests an explanation for the unelongated stable meniscus tip in the stable tip streaming mode; the violent meniscus oscillation and elongation observed in the unstable mode disappear. In addition, the number of drop ejections increases to a maximum in the stable tip streaming mode. This also explains the appearance of the cone jet in low frequency ac electrospays [5]: In the limit of increasing viscous forcing with decreasing f , we postulate the recovery of a steady sharp Taylor cone. In addition, we note that the lower frequency for which the ejection sets occur due to vibration at the macroscopic length scale of the drop meniscus, f_1 , can be associated with f_i for the drop, obtained by a balance between capillary and inertia forces, the latter scaling as $\rho R^2/\mathcal{T}^2$, with \mathcal{T} being the relevant time scale [9]. Careful examination of Fig. 3 indicates that the microjet ejection mode is a transition between the tip streaming and wetting modes: As f increases, the number of drops ejected from the microjet decreases therefore approaching a single periodic ejection with frequency f_1 , i.e., $f_2 \rightarrow f_1$.

The wetting modes, on the other hand, are monoperoiodic, where drop pinch-off occurs at frequency f_1 . The wetting phenomena can be explained by consideration of the Maxwell-Wagner polarization mechanism, embodied by Eq. (1). Figure 4 illustrates the magnitude of the real and imaginary parts of f_{CM} as a function of f . We note the existence of a *crossover frequency*, f_c ,

$$f_c = \frac{1}{2\pi} \sqrt{\frac{(\kappa_o - \kappa_l)(2\kappa_o + \kappa_l)}{(\epsilon_o - \epsilon_l)(2\epsilon_o + \epsilon_l)}} \quad (2)$$

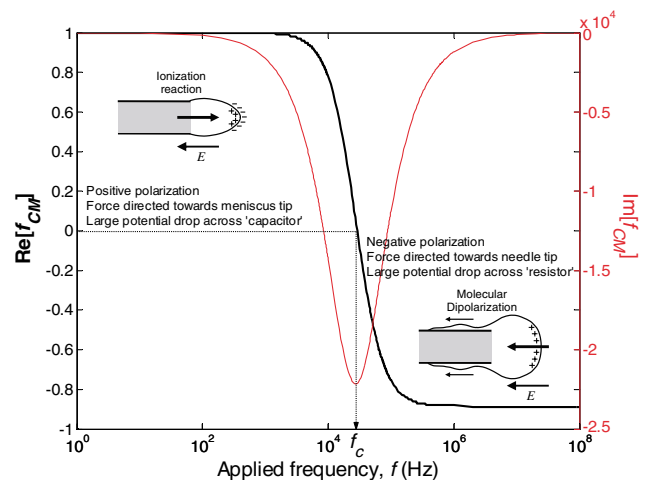


FIG. 4 (color online). Real and imaginary parts of the Clausius-Mossotti factor f_{CM} for ethanol and air as a function of the applied field frequency indicating the positive and negative polarization regions separated by the crossover frequency f_c .

where the sign of $\text{Re}[f_{\text{CM}}]$ reverses. If the electric field is oriented towards the needle tip, molecular polarization bestows a net positive charge at the surface as illustrated in Fig. 4. Nevertheless, despite the change in the orientation of the electric field in every half ac cycle, the Maxwell stress remains oriented in the direction of the needle tip thus flattening the drop around the orifice and causing liquid to recede up the needle as an apparent electrowetting effect, which, in turn, suppresses drop pinch-off. This was confirmed by experiments with a low conductivity fluid such as toluene ($\kappa < 10^{-12}$ S/m, $f_c \sim 5$ kHz), which resulted in severe wetting where drop pinch-off was completely suppressed. However, this effect is observed only at frequencies above f_c (~ 30 kHz) when there is insufficient time for interfacial ionization reaction to occur. Below f_c , interfacial reaction charging is dominant therefore producing an excess of negative ions at the interface. This results in an oppositely directed force which acts to stretch the drop, thus giving rise to tip streaming and microjet ejection.

Both the dependence of the onset voltage on f in Fig. 2 as well as the onset of wetting to produce the drop pinch-off mechanism are consistent with the Maxwell-Wagner polarization mechanism. In this mechanism, the drop can be represented by a simple parallel resistor-capacitor circuit; the buildup of charges due to the interfacial ionization reaction acts like a dielectric capacitor of capacitance C , whereas the ionization reaction can be represented by a Faradaic reaction resistor of resistance \mathcal{R} . A larger potential drop across the capacitor at low f results in positive polarization whereas insufficient time for the reaction to occur leads to a larger potential drop across the resistor at high f . The latter results in negative polarization and hence wetting. The Maxwell stress, τ_n , thus reverses direction at f_c ; we note that f_c in Eq. (2) is associated with the relaxation time of the polarization as the applied field reverses, i.e., $f_c \sim 1/\mathcal{R}C$. From our measurements, we estimate $\mathcal{R} \sim 2$ M Ω and $C \sim 10$ pF, corresponding to a $\mathcal{R}C$ relaxation frequency, $f_{\mathcal{R}C} \sim 1/\mathcal{R}C$, of around 200 kHz, consistent with the observation of complete wetting at V_c . However, wetting also occurs at frequencies other than $f_{\mathcal{R}C}$ and at voltages beyond V_c . This may be due to threshold voltages for ionization or for electrowetting. Nevertheless, it is quite reasonable that the Maxwell-Wagner electric Maxwell stresses, both towards the tip which causes drop ejection and in the opposing direction which causes wetting, reach a maximum when $f \sim f_{\mathcal{R}C}$. When $f \ll 1/\mathcal{R}C$, there is maximum meniscus polarization p at the tip due to the excessive ions produced by the interfacial reaction that also screens the normal field E_n . Since $\tau_n = pE_n$, τ_n is expected to decrease as f decreases. When $f \gg 1/\mathcal{R}C$,

there is considerably less polarization and screening that again leads to a decrease in τ_n . The optimum frequency, $f_{\mathcal{R}C}$, where τ_n is maximum, therefore explains the minimum on the onset voltage at 180 kHz in Fig. 2.

Both f_c and $f_{\mathcal{R}C}$ can also be related to the Maxwell-Wagner polarization time, T_p , given by

$$T_p = \frac{\epsilon_l + 2\epsilon_o}{\kappa_l + 2\kappa_o}, \quad (3)$$

which corresponds to a frequency, f_p , of order 100 kHz. Thus, f_p which lies between f_c and $f_{\mathcal{R}C}$, provides an estimate at which the onset of wetting at f_c completely suppresses the tip streaming and microjet ejections, i.e., where $f_2 \rightarrow f_1$. Despite having allowed for the liquid and air conductivity in our estimation of T_p , it is believed that the associated ac current is not carried by the ions within the ethanol drop but rather by the ions produced by atmospheric or interfacial liquid ionization at the meniscus tip. At very high voltages ($V \gg 6000$ V), corona discharge is observed, causing meniscus elongation and drop ejection to cease, therefore further supporting the postulation that the polarization at the tip involves a current. Although this current produces a net charge at the tip in every half cycle of the applied field, the long drop ejection time scale (10^{-3} s) corresponding to f_1 compared to the period of the applied field stipulates that the ejected drop will remain electroneutral.

*Present address: Department of Chemistry and Biochemistry, National Chung Cheng University, Chia Yi 621, Taiwan.

- [1] J. B. Fenn, M. Mann, C. K. Meng, S. F. Wong, and C. M. Whitehouse, *Science* **246**, 64 (1989).
- [2] J. C. Ijsebaert, K. B. Geerse, J. C. M. Marijnissen, J.-W. J. Lammers, and P. Zanen, *J. Appl. Physiol.* **91**, 2735 (2001).
- [3] J. M. Grace and J. C. M. Marijnissen, *J. Aerosol Sci.* **25**, 1005 (1994); M. Clopeau and B. Prunet-Foch, *J. Aerosol Sci.* **25**, 1021 (1994).
- [4] S. B. Sample and R. Bollini, *J. Colloid Interface Sci.* **41**, 185 (1972); M. Sato, *J. Electrostat.* **15**, 237 (1984).
- [5] J. P. Borra, Y. Tombette, and P. Ehouarn, *J. Aerosol Sci.* **30**, 913 (1999).
- [6] C. D. Eggleton, T.-M. Tsai, and K. J. Stebe, *Phys. Rev. Lett.* **87**, 048302 (2001).
- [7] A. Ramos, H. Morgan, N. G. Green, and A. Castellanos, *J. Phys. D* **31**, 2338 (1998); T. M. Squires and M. Z. Bazant (to be published).
- [8] J. Eggers, *Phys. Rev. Lett.* **71**, 3458 (1993); D. T. Papageorgiou, *Phys. Fluids* **7**, 1529 (1995).
- [9] Y.-J. Chen and P. H. Steen, *J. Fluid Mech.* **341**, 245 (1997).